Wind and Structures, *Vol. 29, No. 4 (2019) 225-234*
DOI: https://doi.org/10.12989/was.2019.29.4.225

Experimental study on aerodynamic characteristics of conductors covered with crescent-shaped ice

Jia-xiang Li[1a], Xing Fu[*2] and Hong-nan Li[2b]

[1]*Department of Civil Engineering, Northeastern University, Shenyang, Liaoning Province, China*
[2]*State Key Laboratory of Coastal and Offshore Engineering, Dalian University of Technology, Dalian, Liaoning Province, China*

(Received September 10, 2018, Revised June 16, 2019, Accepted August 10, 2019)

Abstract. Conductor galloping is a common disaster for the transmission lines. Among the existing analytical methods, the wind tunnel test is highlighted as the most effective approach to obtain the aerodynamic coefficients. In this paper, the aerodynamic coefficients of 12 conductor models covered with the crescent-shaped ice, which were fabricated considering the surface roughness of the iced conductor, were obtained based on the wind tunnel test. The influence of the Reynolds number and the shape parameter β, defined as the ratio of ice thickness to the diameter, were investigated. In addition, the effect of surface roughness of the iced conductor was discussed. Subsequently, unsteady areas of conductor galloping were calculated according to the Den Hartog criterion and the Nigol criterion. The results indicate that the aerodynamic coefficients of iced conductors change sharply at the attack angles of 20° and 170° with the increase of β. The surface roughness of iced conductors changed the range of attack angle, which was influenced by the increase of the Reynolds number. The experimental results can provide insights for preventing and controlling galloping.

Keywords: conductor with crescent-shaped ice; wind tunnel test; shape parameter; Reynolds number; galloping instability

1. Introduction

Galloping is a low-frequency, large-amplitude and self-excited vibration caused by the aerodynamic instability of iced conductors, which can lead to damage to tower members, conductor breaking, and even tower collapses (Ohkuma and Marukawa 2000). Since the 1930s, much attention has been paid to the topic of conductor galloping because of its threat to the operation of the power industry. In 1932, Den Hartog (1932) first explained the vertical mechanism of conductor galloping, in his explanation, galloping was caused by negative damping of the aerodynamic instability. Nigol *et al*. (1981a, b) proposed the torsional theory of galloping, which was based on experimental results. Yu *et al.* (1993a, b) employed perturbation techniques to investigate the non-resonant and resonant galloping of an eccentrically iced conductor and obtained explicit expressions for the periodic and quasi-periodic solutions. Luongo *et al.* (2007, 2008, 2009) studied galloping according to the linear curved-beam theory. Their results demonstrated that the bending effect could not be ignored. Yan *et al.* (2012) improved the Luongo et al.'s work by considering the eccentricity of the iced conductor and analyzed the galloping of two resonant cases analysis. Lou *et al.* (2014) studied the stability of nonlinear galloping of iced transmission lines according to the Routh Hurwitz criterion. Next, they used the center manifold theory and normal form theory to perform bifurcation analysis and obtained an analytic solution, their results of which were verified by numerical simulations. During past three decades, the finite element method (FEM) had been widely used in galloping studies. Desai et al. (1995) used the FEM to establish a multi-span transmission line model to simulate the iced conductor galloping. However, this model is useful only for a single conductor. Zhang *et al*. (2000) proposed a hybrid model to simulate the galloping of bundle conductors based on the Desai et al.'s work. Liu *et al*. (2009) performed a simulation of galloping of a transmission line and found that a new possible galloping mode reflecting the saturation phenomenon could occur. Nevertheless, to study conductor galloping, for either theoretical research or numerical simulations, knowledge of the aerodynamic coefficients of the iced conductor is essential. The quasi-static approach, which assumes that aerodynamic force acting on the moving conductor during the galloping is equal to the force acting on the static conductor, has been verified by many researchers and has been widely adopted for studies of galloping (Denhartog 1932, Desai *et al*. 1996, Desai *et al*. 1995, Lou *et al.* 2014, Nigol and Buchan 1981a, Zhang *et al*. 2000). Up to now, there have been two methods to obtain the aerodynamic coefficients: numerical simulations and wind tunnel tests. Braun and Awruch (2005) obtained the aerodynamic coefficients of bundle conductors while considering the fluid-structure interaction using numerical simulations. Cai *et al*. (2015) calculated the aerodynamic coefficients of iced bundle conductors using the FLUENT. Zhang *et al*. (2015) investigated the dynamic aerodynamic characteristic of an iced conductor, and results demonstrated that the dynamic

[*]Corresponding author, Ph.D.
E-mail: fuxing@dlut.edu.cn
[a] Ph.D.
[b] Ph.D. Professor

http://www.techno-press.com/journals/was&subpage=7
ISSN: 1226-6116 (Print), 1598-6225 (Online)

(a) Long semi-elliptical cross-section (b) Short semi-elliptical cross-section

Fig. 1 The models used in Ma's research

(a) Nigol(Nigol and Buchan 1981b) (b) Farzaneh(Farzaneh *et al*. 2008)

Fig. 2 Ice shapes obtained from icing tests

aerodynamic coefficients were larger than the static ones. There are many advantages associated with the use of numerical simulations to obtain the aerodynamic coefficients of iced conductors, such as low cost and high efficiency. Yet, a comparison with the data obtained from numerical simulations and the wind tunnel tests demonstrated that results from numerical simulations reflected only the varied tendency of the aerodynamic coefficients, but the accuracy was not ideal, and the error in the range of attack angle in which the aerodynamic coefficients varied rapidly was significant (Wang *et al.* 2011). Therefore, wind tunnel tests are the most reliable method to obtain the aerodynamic coefficients of iced conductors.

Because the process of ice formation on a conductor is complicated and influenced by many factors, such as the wind direction, temperature and humidity, the ice shapes are usually irregular. Existing studies have indicated that “D shape”, crescent and sector shapes, are found to be the most common iced shapes that easily lead to conductor galloping (Gu *et al.* 2009, Ma *et al*. 2010, Wang *et al.* 2011). Wang *et al.* (2011) studied the turbulence effect on the aerodynamic characteristics of iced conductor with the crescent-shaped ice or D-shaped ice. Yan *et al.* (2014) investigated the influence of turbulence on the aerodynamic characteristics of bundle conductor with the D-shaped ice or crescent-shaped ice. Li *et al*. (1995, 2000) performed a series of wind tunnel tests to investigate the static and dynamic aerodynamic characteristics of the conductor with the D-shaped or sector-shaped ice. Lou *et al.* (2014) studied the aerodynamic force characteristics of bundle conductors with crescent-shaped or D-shaped ice by wind tunnel tests, and found that sub-conductors had different galloping response patterns when interference effects of aerodynamic force coefficients of sub-conductors were considering during the galloping simulation. In this paper, the wind tunnel tests are performed to investigate the aerodynamic characteristics of conductors with the crescent-shaped ice.

Recent research has demonstrated that the shape parameter has a significant effect on the aerodynamic characteristics (Alonso and Meseguer 2006, Alonso *et al*. 2007, Alonso *et al*. 2010, Ibarra *et al*. 2014). A conductor with the crescent-shaped ice is also called an iced conductor of quasi-oval section or semi-elliptical section. Ma *et al.* (2010) studied the shape parameter for this type of iced conductor. However, their study focused on given attack angles. To investigate the aerodynamic characteristics of conductor with the crescent-shaped ice, the influence of shape parameter on the aerodynamic characteristics must be studied.

When the crescent-shaped ice on the conductor is thin, with an ice thickness of less than 10 mm, the section of iced conductor is similar to a circle. To the knowledge of the author, very few studies refer to galloping of a conductor with thin ice (Hairuo *et al*. 2013, Mccomber and Paradis 1998). Macdonald *et al.* (2006, 2015) studied the mechanism of dry galloping for a circular cylinder, and results indicated that the Reynolds number effect was the reason for the vibration. Many studies have investigated the effect of the Reynolds number on the aerodynamic characteristics for a circular cylinder (ESDU 1980, Ma *et al*. 2015b). Those results showed that an asymmetric pressure distribution occurs within the specific Reynolds number ranges, leading to the appearance of a lift force and a decrease in the drag force, such a phenomenon could cause galloping. Ma *et al.* (2015a) revealed the effect of the Reynolds number on the aerodynamic characteristics of a cylinder with different semi-elliptical cross sections by measuring the wind pressure distribution in a wind tunnel. Their results indicated that the Reynolds number had a great effect on the aerodynamic characteristics when the attack angle is in the range of 0-30° or 150°-180°. But, the iced conductor models used in Ma’s tests, which are shown in Fig. 1, cannot accurately reflect real iced conductors.

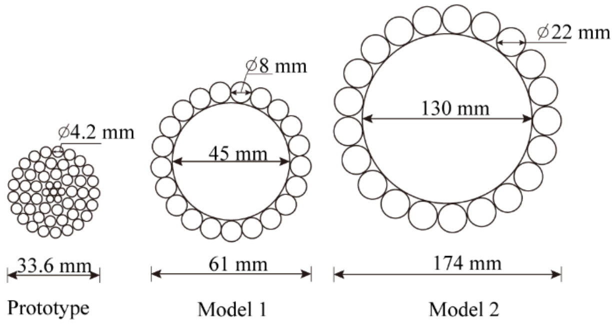

(a) Schematics of the prototype and manufactured models

(b) Real products of the prototype and manufactured models

Fig. 3 Prototype and models of the conductor

To obtain real ice shapes on the conductor, Nigol and Buchan (1981a, b) performed a series of icing tests. Their results are in agreement with the research of Farzaneh *et al*. (2008). The ice shapes obtained in these tests are illustrated in Fig. 2.

From Fig. 2, it is obvious that the ice forms on the windward side, while no ice forms on the leeward side. Although the surface of an iced conductor without ice is not smooth, in many papers, the surface roughness of iced conductor is not taken into account (Gu *et al.* 2009, Ma *et al.* 2015a, Wang *et al*. 2011). The work of Engineering Sciences Data Unit (ESDU) illustrated that the surface roughness of conductor has a great influence on the aerodynamic characteristics (ESDU 1980).

A review of the above-mentioned papers indicates that it is necessary to perform the wind tunnel tests to study the influence of shape parameter and the Reynolds number on the aerodynamic characteristics of a conductor with the crescent-shaped ice. In addition, the influence of surface roughness of iced conductor should be taken into account. Section 2 introduces the experimental setup, and then investigations of influences of shape parameter and the Reynolds number are described in section 3. Finally, section 4 concludes the study.

2. Experimental models and setup

2.1 The iced conductor models

The prototype of conductor used in this paper is LGJ630/45, which is composed of 7 steel cores of 2.8 mm diameter and 45 aluminum strands of 4.2 mm diameter. The dimensional parameters of conductor are listed in Table 1.

The ratio of the outermost aluminum wire diameter over the conductor diameter is 0.13. The aerodynamic characteristics of the iced conductor, with the Reynolds number in the range of 45800-200000, are discussed. To measure the large range of Reynolds number, two conductor models were designed; they are made of aluminum tubes as the core and an outer layer of rubber wires, which were wound tightly onto the tubes (Chadha and Jaster 1975, Liu *et al.* 2012, Zhou *et al.* 2016). The smaller conductor model with the diameter of 61 mm was made of 45-mm aluminum tubes with 8-mm rubber wires. The larger model with the diameter of 174 mm was made of 130-mm aluminum tubes with 22-mm rubber wires. The ratios between the diameters of rubber wire and the conductor were 0.13 for the two models. Fig. 3 shows the details of the prototype conductor and the two manufactured conductor models.

The crescent-shaped ice models, which were made of wood, were connected to the conductor models by bolts. An image of some of ice models is shown in Fig. 4(a). In addition, a diagram of the iced model is illustrated in Fig. 4 (b), where d is the diameter of conductor model and h is the ice thickness. Ice models of different shape parameters, β, which is defined as $\beta=h/d$, were fabricated, as listed in Table 2. Moreover, the lengths of all these models, including the conductor models and the ice models, were 1 m.

Table 1 Parameters of the conductor

Type	Area (mm^2)	Diameter (mm)
LGJ630/45	666.55	33.6

Table 2 Ice models with different β

Number	Conductor model	β
A	Model 1	0.1
B	Model 1	0.2
C	Model 1	0.3
D	Model 1	0.4
E	Model 1	0.5
F	Model 1	0.6
G	Model 1	0.7
H	Model 1	0.8
I	Model 1	0.9
J	Model 1	1.0
K	Model 2	0.1
L	Model 3	0.2

(a) Ice models

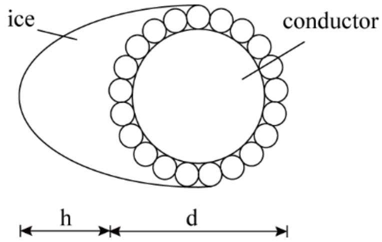

(b) Schematic diagram of the iced conductor model

Fig. 4 Ice models used in the experiments

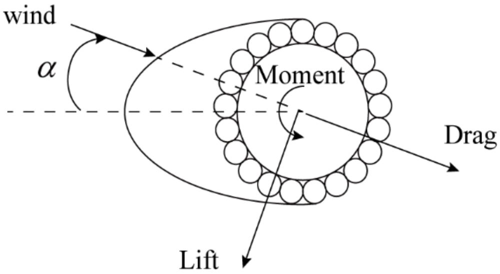

Fig. 5 Attack angle definition

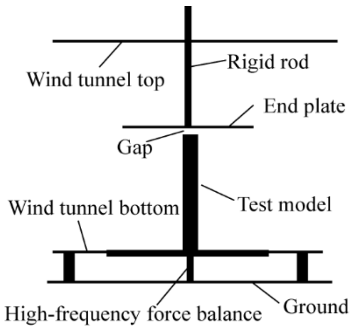

(a) Diagram of the test

(b) The smaller model

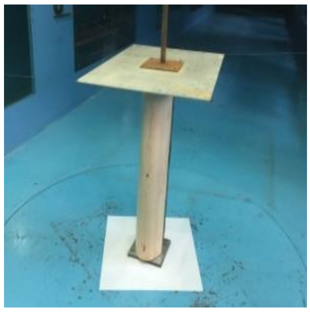

(c) The larger model

Fig. 6 Iced conductor models in the wind tunnel

2.2 The experimental setup

Experiments were conducted in the DUT-1 wind tunnel at Dalian University of Technology, which is a circumfluence closed boundary layer wind tunnel with a working section of 3 m in width, 2.5 m in height, and 18 m in length. The maximum wind velocity is 50 m/s.

To measure the lift force, drag force and moment acting on the iced conductor models, high-frequency force balances were used in the tests. Because the conductor models have large differences in weight, two different types of force balances, 45E12A-163-EF and 75E20A-1125-EF, were adopted. 45E12A-163-EF was used to measure the aerodynamic forces for the smaller model. Its measurement ranges for the horizontal force, vertical force and moment are 100 N, 200 N and 12 N•m, respectively. 75E20A-1125-EF was used to measure the aerodynamic forces for the larger model of an iced conductor and its measurement ranges for the horizontal force, vertical force and moment are 315 N, 630 N and 63 N•m, respectively. The attack angle is defined in Fig. 5. During the tests, the force balances were placed in the center of the rotary table and connected to the bottom of the iced conductor model. The rotary table was controlled to turn around to change the attack angle. To ensure the two-dimensions flow and eliminate the effect of the fluid separation in the end, a steel end plate was installed on the upper end of the iced conductor model, as shown in Fig. 6, with a small gap maintained between the plate and the model. The data from the balances were sampled at a rate of 200 Hz for 30 s at each attack angle, and the attack angle was ranged from 0° to 180° with an increment of 10°.

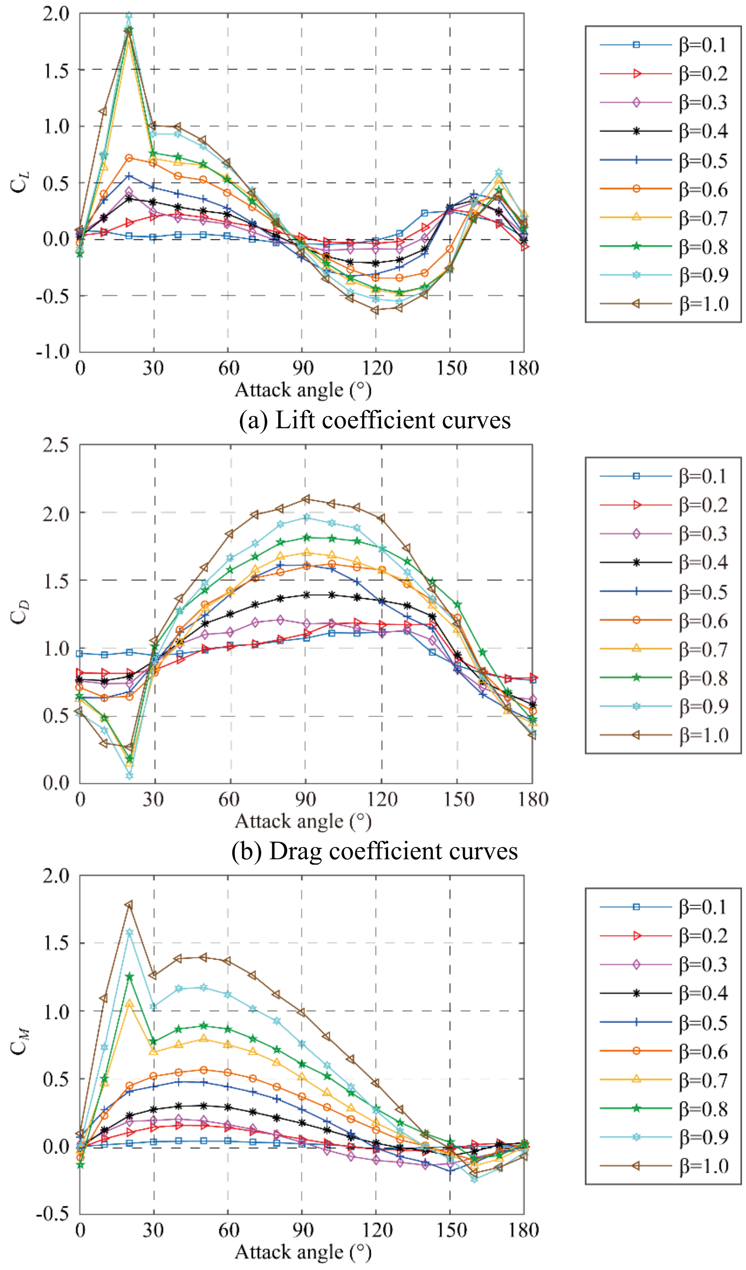

Fig. 7 Aerodynamic coefficient curves for different shape parameters

3. Experimental results

The lift force F_L, drag force F_D and moment F_M obtained through the wind tunnel test can be converted into non-dimensional aerodynamic coefficients, which are defined as follows

$$C_L(\alpha) = \frac{2F_L(\alpha)}{\rho v^2 dL}$$
$$C_D(\alpha) = \frac{2F_D(\alpha)}{\rho v^2 dL} \qquad (1)$$
$$C_M(\alpha) = \frac{2F_M(\alpha)}{\rho v^2 d^2 L}$$

where C_L, C_D and C_M are the lift, drag and moment coefficients, respectively; ρ is the air density, taken to be 1.29 kg/m^3; d is the conductor diameter, adopting the value of 0.061 m for conductor model 1 and 0.174 m for conductor model 2; L is the length of conductor model taken as1 m; and v is the wind speed.

3.1 The effect of β on the aerodynamic characteristics

Fig. 7 shows the variation of aerodynamic coefficients against the attack angles from 0 to 180° for iced conductor models with 10 different β, which increased by 0.1 from 0.1 to 1. Fig. 7(a) reveals that, with the increase of β, there are peak values at the attack angle of 20° and negative slopes in the range from 20° to 120° for the lift coefficient curves; in the ranges of attack angle from 0 to 90° and 170° to 180°, the lift coefficients increase; while the lift coefficients decrease in the range of attack angle from 90° to 170°. In addition, when $\beta \geq 0.7$, the peak values at 20° attack angle increase sharply. Moreover, the magnitudes of negative slope increase sharply around 20°. The most affected range of aerodynamic lift coefficient curves are in the range of 0-30°.

The drag curves are plotted in Fig. 7(b). When $\beta \leq 0.6$, the drag coefficient curves are almost symmetric. Once $\beta \geq 0.7$, the drag coefficients decrease rapidly approximately by 20°, and negative peaks form. In addition, there is a trend that in the ranges of attack angle from 0 to 30° and 170° to 180°, the drag coefficients decrease with the increase of β while increasing in the range of attack angle from 30° to 170°. The most affected regions of drag curves are also found to be between 0 and 30°.

Fig. 7(c) indicates a general trend of the moment curves, first increasing and then decreasing. With increasing β, the moment coefficients increase in the ranges of attack angle from 0 to 150° while decreasing in the range of attack angle from 150° to 180°. In particular, for $\beta \geq 0.7$, a sudden increase occurs at an attack angle of 20°, and the values of the moment curves reach the peak values. The most affected ranges of moment curves are still from 0 to 30°.

For theoretical predictions for the galloping areas for the conductors with the crescent-shaped ice, two criteria (the Den Hartog criterion and Nigol criterion) are used here. The 7-degree polynomials are obtained by the data fitting of the aerodynamic lift coefficient curves and the drag coefficient curves and moment coefficient curves, and then the unstable areas are determined using the following two equations

$$\lambda_d = C_D + \frac{\partial C_L}{\partial \alpha} < 0 \tag{2}$$

$$\lambda_n = \frac{\partial C_m}{\partial \alpha} < 0 \tag{3}$$

where λ_d and λ_n are the Den Hartog coefficient and the Nigol coefficient, respectively.

From the theories of Den Hartog galloping and Nigol galloping, the unstable areas for galloping are shown in Fig. 8 and Fig. 9 for the attack angle range from 0° to 180°. Fig. 8 reveals that the galloping could occurs in the attack angle range from 170° to 180° for $0.2 \leq \beta \leq 0.6$. Once $\beta \geq 0.7$, the galloping area will expand, and galloping can also occur approximately from 20° to 50°. The reason for this behavior is that once $\beta \geq 0.7$, the lift coefficient curves suddenly increase at the 20° attack angle, thus leading to large negative slopes. Meanwhile, the drag curves drop at the 20° attack angle. Therefore, the galloping areas become larger. The unstable area from 50° to 131° for β=0.1 are found to expand to the range from 27° to 172° for β=1.0, as shown in Fig. 9. The unstable area obviously increases with β according to the Nigol theory.

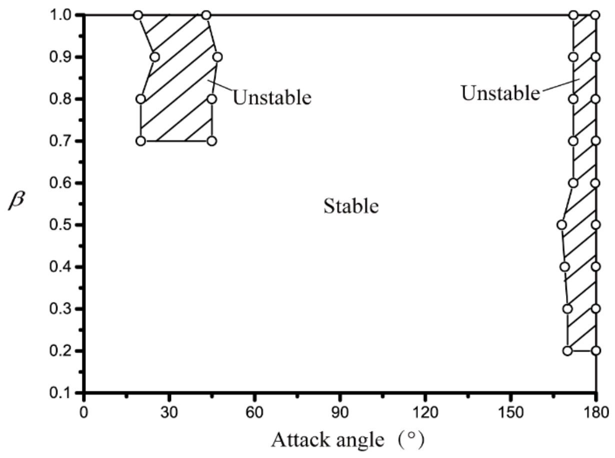

Fig. 8 Den Hartog coefficient for different shape parameters

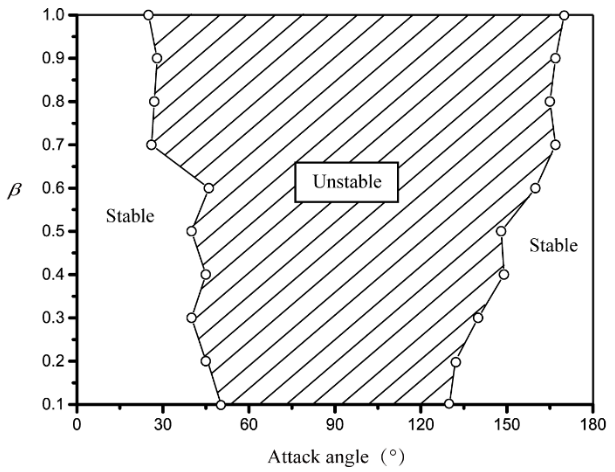

Fig. 9 Nigol coefficient for different shape parameters

3.2 Effect of Reynolds number on the aerodynamic characteristics

The iced conductor models for 2 different values of β are used in this section. The lift coefficient curves for different Reynolds numbers are illustrated in Fig. 10(a). The Reynolds number is observed to have a significant effect on the variation of lift curves when the attack angle is in the range of 0-50° or 110°-140° for the Reynolds number between 45800 and 200000. However, these results are different from the results of Ma *et al.* (2015a). In their work, the aerodynamic characteristics of two different conductors with a crescent-shaped ice, ignoring the surface roughness of conductor models, both varied with increasing Reynolds number for the attack angles of 0-30° or 150°-180°. The differences between the work of Ma *et al.* (2015a) and this paper may be caused by the surface roughness of the models. The Reynolds numbers obviously results in the increasing magnitude of negative slope for the lift coefficient curves in cases in which galloping might occur. From Fig. 10(b), with increases in the Reynolds number, the drag coefficient curves drop sharply for attack angles in the range of 0-50° and 110°-140°, just as the

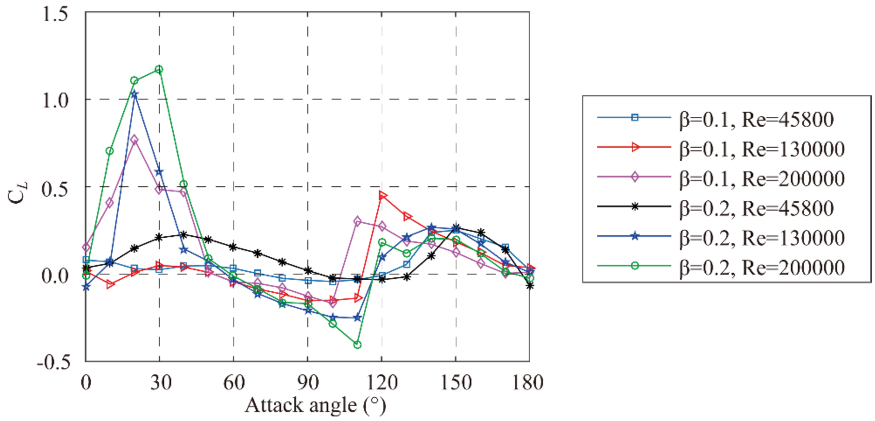

(a) Lift coefficient curves

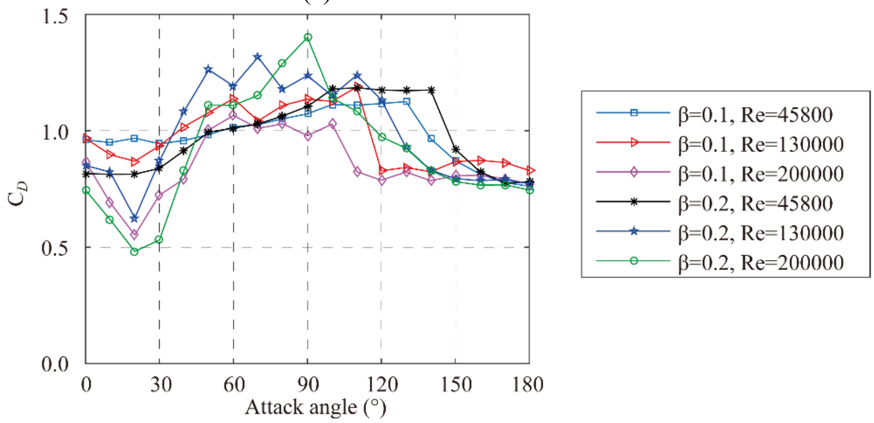

(b) Drag coefficient curves

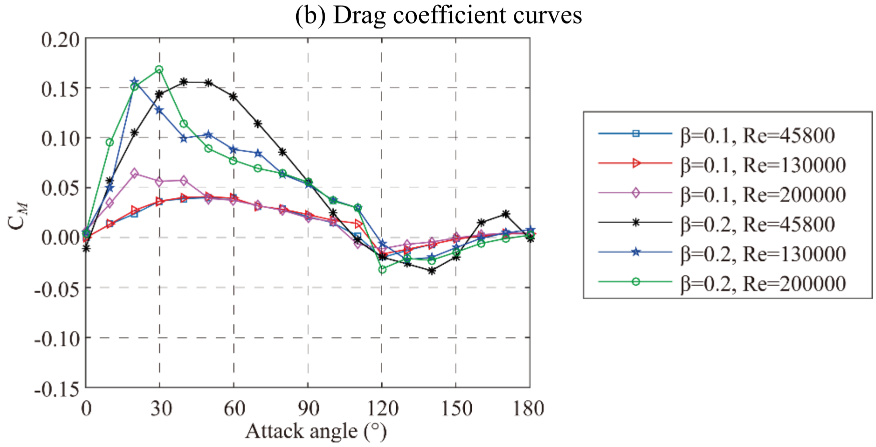

(c) Moment coefficient curves

Fig. 10 Aerodynamic coefficient curves for different Reynolds numbers

variation range of lift coefficient curves is influenced by the Reynolds numbers. Fig. 10(c) indicates that the regions of moment curves are changed because of Reynolds number, and the affected range is the same as the ranges of lift and drag coefficient curves.

In addition, it can be observed that in the case of β=0.1, only when the Reynolds number is 200000 do the aerodynamic coefficient curves change significantly in the ranges of 0°-50° or 110°-140°. For β=0.2, once the Reynolds number is greater than 130000, a significant variation in the aerodynamic curves occurs in the ranges of 0°-50° or 110°-140°. Compared with the two different cases, one can conclude that the higher β leads to a smaller Reynolds number with which the aerodynamic coefficient curves begin to change significantly.

According to Eq. (2), the Den Hartog coefficients were calculated as plotted in Fig.11. In the case of β=0.1, only when the Reynolds number is 200000 is the unstable galloping area observed in the range of 28°-58°. For β=0.2, when the Reynolds number is 130000, the iced conductor may gallop in the range of 29°-55°, and the unstable area expands to the range of 29°-63° when the Reynolds number is 200000. Clearly, the unstable area of galloping increases with the Reynolds number.

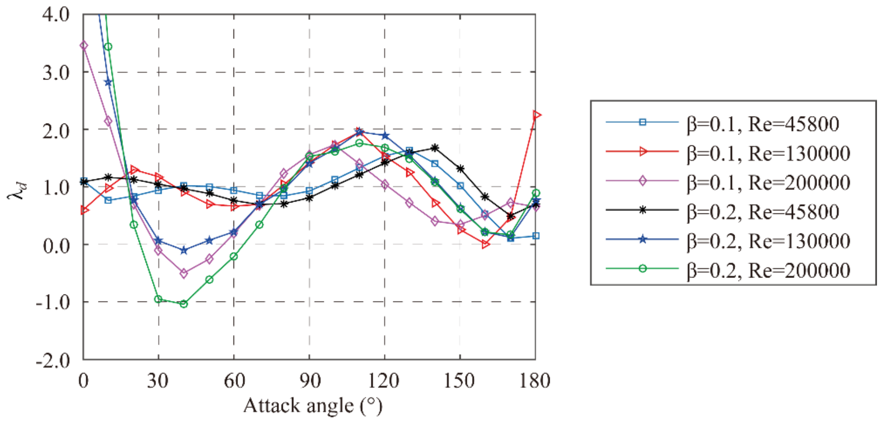

Fig. 11 Den Hartog coefficients for different Reynolds numbers

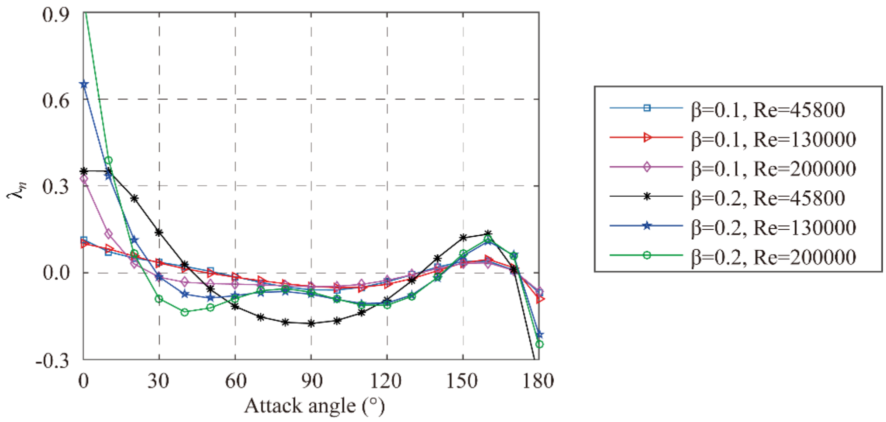

Fig. 12 Nigol coefficients for different Reynolds numbers

The Nigol coefficient curves are shown in Fig. 12. The dangerous areas for galloping are found to increase with both the Reynolds number and β. By comparing the results with the unstable areas obtained by the Den Hartog theory, the Nigol unstable areas are found to be much larger than the Den Hartog unstable areas. Furthermore, when the Reynolds number is small, galloping may occur according to the Nigol theory. Therefore, a single conductor with the thin crescent-shaped ice can easily exhibit galloping according to the Nigol theory. In addition, the galloping of thin iced bundle conductors with consideration of surface roughness should be studied in the future.

4. Conclusions

In this paper, the aerodynamic characteristics of iced conductors with different shape parameters and Reynolds numbers were studied using wind tunnel tests. In addition, the effect of surface roughness was discussed. The following conclusions are drawn as:

- For the conductor with a crescent-shaped ice, the shape parameter β has a significant influence on the aerodynamic characteristics. With increasing β, the aerodynamic curves change significantly in the range of 0-30°, and these changes can lead to expansion of instability areas according to both Den Hartog theory and Nigol theory.
- For a conductor with the crescent-shaped ice, a larger value of β results in a smaller Reynolds number with which the aerodynamic coefficient curves begin to change significantly. In addition, with increasing Reynolds number, the aerodynamic curves change significantly in the range of 0-30° and 110°-140°, leading to the increasing of the instability area.
- The surface roughness of iced conductor has a considerable effect on the attack angle ranges, which are influenced by the increasing the Reynolds number. As a result, the surface roughness should be taken into account.
- The instability areas calculated according to both the Den Hartog theory and Nigol theory increase with the Reynolds number.

Acknowledgments

The research described in this paper was financially supported by the National Natural Science Foundation of China (grant nos. 51808100 and 51421064), the Fundamental Research Funds for the Central Universities (grant nos. N170103014 and N170108029, and DUT19RC(4)021)), the China Postdoctoral Science Foundation (grant no 2018M631808) and the Postdoctoral Foundation of Northeastern University (grant no. 20190319).

References

Alonso, G. and Meseguer, J. (2006), "A parametric study of the galloping stability of two-dimensional triangular cross-section bodies", *J. Wind Eng. Ind. Aerod*., **94**(4), 241-253. https://doi.org/10.1016/j.jweia.2006.01.009.

Alonso, G., Meseguer, J. and Pérez-Grande, I. (2007), "Galloping stability of triangular cross-sectional bodies: A systematic approach",. *J. Wind Eng. Ind. Aerod*., **95**(2007), 928-940. https://doi.org/10.1016/j.jweia.2007.01.012.

Alonso, G., Meseguer, J., Sanz-Andrés, A. and Valero, E. (2010), "On the galloping instability of two-dimensional bodies having elliptical cross-sections", *J. Wind Eng. Ind. Aerod.*, **98**(8-9), 438-448. https://doi.org/10.1016/j.jweia.2010.02.002.

Braun, A.L. and Awruch, A.M. (2005), "Aerodynamic and aeroelastic analysis of bundled cables by numerical simulation", *J. Sound Vib*., **284** (2005), 51-73. https://doi.org/10.1016/j.jsv.2004.06.026

Cai, M., Yan, B., Lu, X. and Zhou, L. (2015), "Numerical simulation of aerodynamic coefficients of iced quad bundle conductors", *IEEE T. Power Deliver*., **30**(4), 1-1. https://doi.org/10.1109/TPWRD.2015.2417890.

Chadha, J. and
Jaster, W. (1975), "Influence of turbulence on the galloping instability of iced conductors", *IEEE T. Power Appar. Syst*., **PAS-94**(5), 1489-1499. https://doi.org/10.1109/T-PAS.1975.31991.

Denhartog, J.P. (1932), "Transmission line vibration due to sleet", *T. Am. Inst. Electr. Eng*., **51**(4), 1074-1076. https://doi.org/10.1109/T-AIEE.1932.5056223.

Desai, Y.M., Yu, A.H.S. and Popplewell, N. (1996), "Perturbation based finite element analyses of transmission line galloping", *J. Sound Vib*., **191**(4), 469-489. https://doi.org/10.1006/jsvi.1996.0135.

Desai, Y.M., Yu, P., Popplewell, N. and Shah, A.H. (1995), "Finite element modelling of transmission line galloping", *Comput. Struct*., **57**(3), 407-420. https://doi.org/10.1016/0045-7949(94)00630-L.

ESDU (1980), "Mean Forces, Pressures and Flow Field Velocities for Circular Cylindrical Structures: Single Cylinder with Two-dimensional Flow", Engineering Sciences Data Unit, London, England.

Farzaneh, M., Volat, C. and Leblond, A. (2008), "Anti-icing and de-icing techniques for overhead lines", Springer Netherlands, Dordrecht, South Holland, Holland.

Gu, M., Ma, W., Quan, Y. and Huang, P. (2009), "Aerodynamic force characteristics and stabilities of two typical iced conductors", *J. Tongji Univ*., **37**(10), 1328-1332. https://doi.org/10.3969/j.issn.0253-374x.2009.10.010.

Li, Hairuo, Guo, H. and Xie, Q. (2013), "Wind tunnel test on aerodynamic characteristic of conductor with thin ice accretions", *Electr. Power Constr*., **34**(3), 12-16. https://doi.org/10.3969/j.issn.1000-7229.2013.03.003.

Ibarra, D., Sorribes, F., Alonso, G. and Meseguer, J. (2014), "Transverse galloping of two-dimensional bodies having a rhombic cross-section", *J. Sound Vib*., **333**(13), 2855-2865. https://doi.org/10.1016/j.jsv.2014.02.030.

Li, W.P. (2000), "Dynamic aerodynamic characteristics of the galloping of bundled iced power transmission lines", *Acta Aerodyn. Sin*., **18**(4), 413-420. https://doi.org/10.3969/j.issn.0258-1825.2000.04.006

Li, W.P., Yang, X. and Zhang, L. (1995), "Static aerodynamic characteristics of the galloping of bundled iced power transmission lines", *Acta Aerodyn. Sin*., **13**(4), 427-434.

Liu, X., Yan, B., Zhang, H. and Zhou, S. (2009), "Nonlinear numerical simulation method for galloping of iced conductor", *Appl. Math. Mech*., **30**(4), 489-501. https://doi.org/10.1007/s10483-009-0409-x.

Liu, X.H., Bo, Y., Zhang, H.Y. and Song, Z. (2012), "Numerical investigation on galloping of iced quad bundle conductor in stochastic wind field", *IEEE T. Power Deliver*., **27**(2), 784-792. https://doi.org/10.1109/TPWRD.2012.2185252

Lou, W., Yang, L., Huang, M. and Yang, X. (2014), "Two-parameter bifurcation and stability analysis for nonlinear galloping of iced transmission lines", *J Eng. Mech*., **140**(11), 04014081. https://doi.org/10.1061/(ASCE)EM.1943-7889.0000795.

Lou, W., Lv, J., Huang, M., Yang, L. and Yan, D. (2014), "Aerodynamic force characteristics and galloping analysis of iced bundled conductors", *Wind Struct*., **18**(2), 135-154. DOI: https://doi.org/10.12989/was.2014.18.2.135

Luongo, A., Zulli, D. and Piccardo, G. (2007), "A linear curved-beam model for the analysis of galloping in suspended cables", J. Mech. Mater. Struct., **2**(4), 675-694. https://doi.org/10.2140/jomms.2007.2.675.

Luongo, A., Zulli, D. and Piccardo, G. (2008), "Analytical and numerical approaches to nonlinear galloping of internally resonant suspended cables", *J. Sound Vib*., **315**(3), 375-393. https://doi.org/10.1016/j.jsv.2008.03.067.

Luongo, A., Zulli, D. and Piccardo, G. (2009), "On the effect of twist angle on nonlinear galloping of suspended cables", *Comput. Struct*., **87**(2009), 1003-1014. https://doi.org/10.1016/j.compstruc.2008.04.014.

Ma, W., Gu, M., Quan, Y. and Huang, P. (2010), "Testing study on aerodynamic force characteristics of quasi-oval shape iced conductor", *J. Tongji Univ*., **38**(10), 1409-1413. https://doi.org/10.3969/j.issn.0253-374x.2010.10.002

Ma, W.Y., Liu, Q.K., Du, X.Q. and Wei, Y.Y. (2015a), "Effect of the Reynolds number on the aerodynamic forces and galloping instability of a cylinder with semi-elliptical cross sections", *J. Wind Eng. Ind. Aerod*., **146**(2015), 71-80. https://doi.org/10.1016/j.jweia.2015.08.006.

Ma, W.Y., Yuan, X.X., Zhang, X.B., Wei, Y.Y. and Liu, Q.K. (2015b), "Characteristics of aerodynamic forces on a cylinder at Reynolds numbers from 35k to 330k", *Eng. Mech*., **32**(1), 348-352. https://doi.org/10.6052/j.issn.1000-4750.2014.05.S022

Macdonald, J. and Larose, G.L. (2006), "A unified approach to aerodynamic damping and drag/lift instabilities, and its application to dry inclined cable galloping", *J. Fluid. Struct*., **22**(2), 229-252. https://doi.org/10.1016/j.jfluidstructs.2005.10.002.

Mccomber, P. and Paradis, A. (1998), "A cable galloping model for thin ice accretions", *Atmos. Res*., **46**(1), 13-25. https://doi.org/10.1016/S0169-8095(97)00047-1.

Nigol, O. and Buchan, P.G. (1981a), "Conductor galloping-Part II torsional mechanism", *IEEE T. Power Appar. Syst*., **PAS-100**(2), 708-720. https://doi.org/10.1109/TPAS.1981.316922

Nigol, O. and Buchan, P.G. (1981b), "Conductor galloping Part I - Den Hartog mechanism", *IEEE T. Power Appar. Syst*., **PAS-100**(2), 699-707. https://doi.org/10.1109/TPAS.1981.316921.

Nikitas, N. and Macdonald, J.H.G. (2015), "Aerodynamic forcing characteristics of dry cable galloping at critical Reynolds numbers", *Eur. J. Mech*., **49**(2015), 243-249. https://doi.org/10.1016/j.euromechflu.2014.09.005.

Ohkuma, T. and Marukawa, H. (2000), "Galloping of overhead transmission lines in gusty wind", *Wind Struct.*, **3**(4), 243-253.

https://doi.org/10.12989/was.2000.3.4.243.
Wang, X., Lou, W.J., Shen, G.H. and Fu-You, X.U. (2011), "A wind tunnel study on aerodynamic characteristics of iced conductor", *Acta Aerodyn. Sin*., **29**(5), 573-579. https://doi.org/110.3969/j.issn.0258-1825.2011.05.007.
Yan, D., LV, Z., Lin, W. and Lou, W. (2014), "Experimental study on effect of turbulence intensity on the aerodynamic characteristics of iced conductors", *High Volt. Eng*., **40**(2), 450-457. https://doi.org/10.13336/j.1003-6520.hve.2014.02.017
Yan, Z., Yan, Z., Li, Z. and Tan, T. (2012), "Nonlinear galloping of internally resonant iced transmission lines considering eccentricity", *J. Sound Vib*., **331**(15), 3599-3616. https://doi.org/10.1016/j.jsv.2012.03.011.
Yu, P., Desai, Y.M., Popplewell, N. and Shah, A.H. (1993a), "Three-degree-of-freedom model for galloping. Part II: solutions", *J. Eng. Mech*., **119**(12), 2426-2448. https://doi.org/10.1061/(ASCE)0733-9399(1993)119:12(2426).
Yu, P., Desai, Y.M., Shah, A.H. and Popplewell, N. (1993b), "Three-degree-of-freedom model for galloping. Part I: formulation", *J. Eng. Mech*., **119**(12), 2404-2425. https://doi.org/10.1061/(ASCE)0733-9399(1993)119:12(2404).
Zhang, Q., Popplewell, N. and Shah, A.H. (2000), "Galloping of bundle conductor", *J. Sound Vib*., **234**(1), 115-134. https://doi.org/10.1006/jsvi.1999.2858.
Zhang, Z., Yang, X.P. and Hao, S.Y. (2015), "Numerical simulation and analysis of dynamic aerodynamic characteristics of iced conductor", *J. Vib. Shock*, **34**(7), 209-214. https://doi.org/10.13465/j.cnki.jvs.2015.07.033.
Zhou, L., Yan, B., Zhang, L. and Zhou, S. (2016), "Study on galloping behavior of iced eight bundle conductor transmission lines", *J. Sound Vib.*, **362**(2016), 85-110. https://doi.org/10.1016/j.jsv.2015.09.046.

CC